Understanding the Steric Control of Stereoselective Olefin Binding in Cyclopentadienyl Complexes of Rhenium: An Application of de Novo Ligand Design

Aaron M. Gillespie and David P. White*

Department of Chemistry, University of North Carolina at Wilmington, 601 South College Road, Wilmington, North Carolina 28403-3297

Received June 6, 2001

Gladysz has demonstrated that the $[(\eta^5\text{-}C_5H_5)Re(NO)(PPh_3)]^+$ fragment can stereoselectively bind prochiral olefins. The origins of selectivity are thought to be rooted in the steric interaction between the substituent on the olefin and ligands on the Re. Using Brown's ligand repulsive energy methodology, we have verified that stereoselectivity toward prochiral α-olefins in $[(\eta^5\text{-}C_5H_5)Re(NO)(PPh_3)]^+$ can be understood in terms of a steric argument. Using molecular mechanics, we examine how the fragment $[(\eta^5\text{-}C_5R_5)Re(NO)(L)]^+$ (R = H, Me; L = PMe_3, PPh_3) stereoselectively binds prochiral α-olefins, CH_2=CHR (R = Me, *n*-Pr, CH_2Ph, Ph, *i*-Pr, *t*-Bu, and $SiMe_3$). We have used the molecular mechanics results to rate the relative impact on stereoselectivity toward α-olefins by the size of the cyclopentadienyl ring versus the size of the phosphine.

Introduction

Chiral recognition between an enantiomerically pure organometallic complex and a prochiral moiety is an important theme in contemporary organometallic chemistry. Much computational work has been devoted to this type of problem, particularly applied to important reactions such as asymmetric hydrogenation and olefin polymerization.[1−12] Most of the current approaches to modeling organometallic processes involve using a single computational method to study an array of structures. Recently, Cundari has recognized the importance of using different computational methods to design a catalyst that is targeted for a specific transformation, which is called de novo ligand design.[13]

De novo ligand design is a pyramid approach to molecular modeling (Figure 1). The base of the pyramid is molecular mechanics (MM) in which many structures can be generated in a relatively short amount of time. The next level is the computationally more intense semiempirical quantum mechanics (SEQM) calculations in which low-energy molecular mechanics structures are refined. Finally, the small number of low-energy structures that survive SEQM screening are passed to ab initio calculations for accurate geometry optimization and energy determination. In this paper, we present the first step in Cundari's de novo ligand design approach to the modeling of the steric interaction between a prochiral olefin and an enantiomerically pure organometallic Lewis acid.

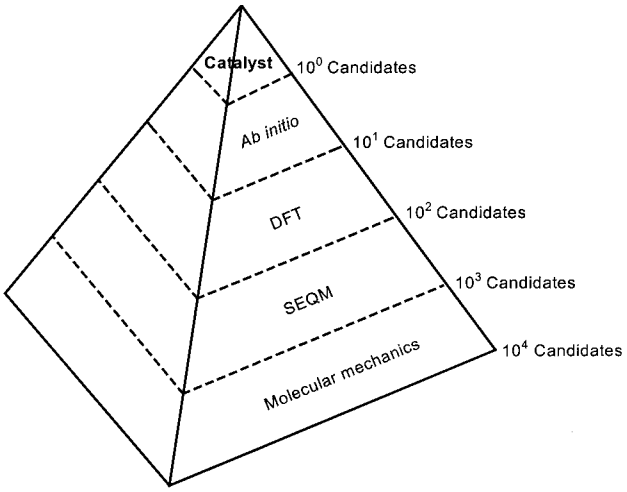

Figure 1. De novo design pyramid: molecular mechanics forms the base of the pyramid since tens of thousands of potential catalysts can be generated because of the speed of computation. Semiempirical quantum mechanics (SEQM) narrows the number of candidates to thousands. Density functional theory (DFT) and ab initio computations further narrow the total number of candidates to give the single, well-designed catalyst.

(1) Castonguay, L. A.; Rappé, A. K. *J. Am. Chem. Soc.* **1992**, *114*, 5832−5842.
(2) Rappé, A. K.; Colwell, K. S.; Casewit, C. J. *Inorg. Chem.* **1993**, *32*, 3438−3450.
(3) Rappé, A. K.; Casewitt, C. J. *Molecular Mechanics across Chemistry*; University Science Books: Sausalito, 1997.
(4) Landis, C. R.; Halpern, J. *Organometallics* **1983**, *2*, 840−842.
(5) Landis, C. R.; Halpern, J. *J. Am. Chem. Soc.* **1987**, *109*, 1746−1754.
(6) McCulloch, B.; Halpern, J.; Thompson, M. R.; Landis, C. R. *Organometallics* **1990**, *9*, 1392−1395.
(7) Giovannetti, J. S.; Kelly, C. M.; Landis, C. R. *J. Am. Chem. Soc.* **1993**, *115*, 4040−4057.
(8) Landis, C. R.; Root, D. M.; Cleveland, T. In *Reviews in Computational Chemistry*; Lipkowitz, K. B., Boyd, D. B., Eds.; VCH: New York, 1995; Vol. 6, pp 73−381.
(9) Landis, C. R.; Hilfenhaus, P.; Feldgus, S. *J. Am. Chem. Soc.* **1999**, *121*, 8741−8754.
(10) Landis, C. R.; Feldgus, S. *Organometallics* **2001**, *11*, 2374−2387.
(11) Comba, P.; Hambley, T. W. *Molecular Modeling of Inorganic Compounds*; VCH: New York, 1995.
(12) White, D. P.; Douglass, W. In *Computational Organometallic Chemistry*; Cundari, T. R., Ed.; Marcel-Dekker: New York, 2001; pp 237−275.
(13) Buda, C.; Cundari, T. R.; Shenkin, P. S. *Inorg. Chem.*, submitted.

10.1021/om010481a CCC: $20.00
Publication on Web 10/26/2001

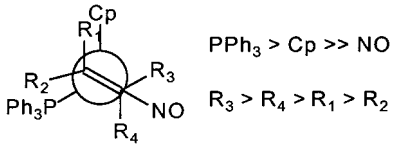

Figure 2. Newman projection of $[(\eta^5\text{-}C_5H_5)Re(\eta^2\text{-olefin})(PPh_3)(NO)]^+$ as viewed down the olefin centroid−Re axis.

Gladysz has shown that the coordinatively unsaturated $[CpRe(NO)(PPh_3)]^+$ (Cp = η^5-C_5H_5) fragment is capable of stereoselectively binding prochiral unsaturated species.[14] In particular, Gladysz proposed that the steric interaction between ligands on the metal and the substituents on the olefin gives rise to the stereodifferentiation between olefinic faces, Figure 2. To understand the binding selectivity, Gladysz recognized that PPh_3 is larger than Cp, which, in turn, is larger than NO. Therefore, the olefin must orient itself so that the largest substituent on the olefin is located in the least sterically congested interstice between the ligands.[14] For a tetrasubstituted olefin, Gladysz concluded that the steric size of the ligands forces the olefin to adopt the orientation shown in Figure 2, which assumes that $R_3 > R_4 > R_1 > R_2$. In short, Gladysz proposes that the steric interplay between ligands and substituents is responsible for the stereoselective olefin binding.

Computational chemistry has been applied to the problem of the quantification of steric effects in organometallic chemistry with a great deal of success.[15−26] In particular, we focus our attention on Brown's ligand repulsive energy methodology.[15] Consider a $Cr(CO)_5L$ complex, in which we wish to determine the steric demand of L. In the geometry-optimized structure, the equilibrium Cr−L bond length is r_e. Ligand repulsive energy, E_R, is defined by the change in van der Waals *repulsive* energy, $E_{vdW,R}$, as a function of Cr−L distance, r, multiplied by the equilibrium Cr−L distance r_e:

$$E_R = -r_e\left(\frac{\partial E_{vdW,R}}{\partial r}\right) \qquad (1)$$

(The negative sign ensures that as the steric bulk of the ligand increases, E_R also increases.) Near the equilibrium distance, r_e, the plot of $E_{vdW,R}$ versus distance is linear. In the original papers, Brown used a modified MMP2 force field energy to compute E_R values for ligands attached to the prototypical $Cr(CO)_5$ fragment.[15,17,27,28] Subsequently, Brown and others have computed ligand repulsive energies with a variety of different ligands in a series of different prototypical environments using two different force fields (MMP2 and UFF).[2,18,22,24,25,29,30] In general, ligand repulsive energies show the same trend irrespective of either fragment or force field used for their computation.[18,22,24,25,29]

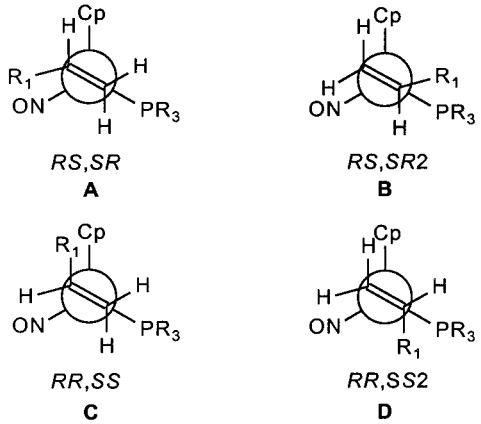

Figure 3. Four different orientations for the binding of a prochiral α-olefin, $CH_2{=}CHR_1$ (R_1 = Me, Bn, Ph, *i*-Pr, *t*-Bu, and $SiMe_3$), to a chiral organometallic fragment, $[(\eta^5\text{-}C_5H_5)Re(NO)(PR_3)]^+$ (R = Me, Ph). Note that the same face of the prochiral olefin is coordinated to the metal in **A** and **B**, and similarly in **C** and **D**.

In this paper, we apply the ligand repulsive energy methodology to the computation of the steric interaction between prochiral α-olefins, $CH_2{=}CHR$ (R = Me, *n*-Pr, CH_2Ph (Bn), Ph, *i*-Pr, *t*-Bu, and $SiMe_3$),[14] and the chiral organometallic fragments, $[CpRe(NO)(L)]^+$ and $[Cp^*Re(NO)(L)]^+$ (L = PPh_3, PMe_3; Cp* = η^5-C_5Me_5). Ligand repulsive energies computed with the $Cr(CO)_5$ fragment are given the label E_R, and other ligand repulsive energies are called $E_R^{\text{Force field}}$(fragment).[15,17,29,24] For convenience, we call the ligand repulsive energies of the η^2-bonded olefins bonded to the cyclopentadienyl rhenium fragments reported in this paper E_R''.

The size difference between PPh_3 and PMe_3 (cone angles of 145° and 118°, respectively)[20] and the size difference between Cp and Cp* (cone angles of 128° and 182°, respectively)[20] will allow us to evaluate whether we observe improved selectivity by modifying the size of the phosphine ligand, which is experimentally facile, or by modifying the size of the cyclopentadienyl ring, which is experimentally tedious.[14] In addition, the isomer with lowest ligand repulsive energy for $[CpRe(NO)(PPh_3)(\eta^2\text{-}CH_2{=}CHR)]^+$ should be the dominant experimental isomer if steric effects control binding selectivity.[14]

Molecular Mechanics Approach. Since there are no MM2 parameters to our knowledge for $[CpRe(NO)(phosphine)]^+$ complexes, and since the trend in ligand repulsive energies for structures generated using MMP2 and UFF is the same,[25] we chose to use the UFF for computations. There are four possible orientations in which a prochiral olefin can bind to an enantiomerically pure $[CpRe(NO)(PPh_3)]^+$ fragment, illustrated in Figure 3.

(14) Gladysz, J. A.; Boone, B. J. *Angew. Chem., Int. Ed. Engl.* **1997**, *36*, 550−583.
(15) Brown, T. L. *Inorg. Chem.* **1992**, *31*, 1286−1294.
(16) Brown, T. L.; Lee, K. J. *Coord. Chem. Rev.* **1993**, *128*, 89−116.
(17) Choi, M.-G.; Brown, T. L. *Inorg. Chem.* **1993**, *32*, 1548−1553.
(18) Choi, M.-G.; Brown, T. L. *Inorg. Chem.* **1993**, *32*, 5603−5610.
(19) Chin, M.; Durst, G. L.; Head, S. R.; Bock, P. L.; Mosbo, J. A. *J. Organomet. Chem.* **1994**, *470*, 73−85.
(20) White, D.; Coville, N. J. *Adv. Organomet. Chem* **1994**, *36*, 95−158.
(21) Woo, T. K.; Ziegler, T. *Inorg. Chem.* **1994**, *33*, 1857−1863.
(22) White, D. P.; Brown, T. L. *Inorg. Chem.* **1995**, *34*, 2718−2724.
(23) Yuriev, E.; Orbell, J. D. *J. Comput.-Aided Mol. Des.* **1996**, *10*, 589−606.
(24) White, D. P.; Anthony, J. C.; Oyefeso, A. O. *J. Org. Chem.* **1999**, *64*, 7707−7716.
(25) Bubel, R. J.; Douglass, W.; White, D. P. *J. Comput. Chem.* **2000**, *21*, 239−246.
(26) White, D. P. In *Computational Organometallic Chemistry*; Cundari, T. R., Ed.; Marcel-Dekker: New York, 2001; pp 39−69.
(27) Caffery, M. L.; Brown, T. L. *Inorg. Chem.* **1991**, *30*, 3907−3914.
(28) Lee, K. J.; Brown, T. L. *Inorg. Chem.* **1992**, *31*, 289−294.
(29) Choi, M.-G.; White, D.; Brown, T. L. *Inorg. Chem.* **1994**, *33*, 5591−5594.

Two of the orientations have the same face of the olefin coordinated to the metal. Of these two, one has the olefinic substituent *syn* to the phosphine ligand and one has the substituent *anti* to the phosphine. The choice of P−Re−Centroid−C_{ipso} torsion angle of 0° or 180° is based on electronic structure computations,[31−33] which ensures maximum overlap between olefin LUMO and metal HOMO. Work in the literature has demonstrated that orbital overlap, rather than steric effects, dominates in the determination of the P−Re−Centroid−C_{ipso} torsion angle.[14]

For conformationally flexible olefinic substituents, we anticipate intraligand interactions could influence the overall stereoselectivity of the system. A severely strained interaction between the olefinic substituent, R, and the PPh_3 ligand, in particular, could eliminate several conformers from consideration. When we attempted a Monte Carlo conformational search on the [CpRe(NO)-$(PPh_3)(\eta^2$-CH_2=CHR)]$^+$ complexes using UFF in the four olefin orientations illustrated in Figure 3, all the olefins underwent a face-flip to relieve steric strain. Therefore, we chose to carry out a conformational search of the olefin and the [CpRe(NO)(PPh_3)]$^+$ fragment separately.

The conformational space of [CpRe(NO)(PPh_3)]$^+$ was sampled using a Monte Carlo algorithm in Cerius^2 4.0 using the UFF. Each rotatable bond was allowed to vary simultaneously by a randomly different amount and the resulting structure energy-minimized using the SMART minimizer.[34] A total of 2000 conformers were generated, and the lowest energy one used in all subsequent computations.

It is possible that the free olefin is in a different conformation than the olefin bound to an organometallic moiety. Therefore, we chose to carry out the conformational search of the olefin bonded to the $Cr(CO)_5$ fragment, as used by Brown in the development of the ligand repulsive energy methodology.[15] Brown and White have demonstrated that ligand repulsive energies of olefins in the $Cr(CO)_5$ environment follow the same trends as those in the CpRh(CO) environment.[22] The conformational space of the olefin was sampled using the same method reported previously[22] with the olefin bonded to a $Cr(CO)_5$ fragment in Cerius^2 4.5[35] and the modified MMP2 force field employed.[22] When there are few conformational degrees of freedom, a grid search was carried out with a 1° grid space. If the grid search produced more than 2000 conformers, then a Monte Carlo algorithm was employed and the torsion angles for all rotatable bonds were simultaneously varied by randomly different amounts to generate 2000 conformers.[22] In all cases, the lowest energy conformer was selected and bonded to the [CpRe(NO)(PPh_3)]$^+$ fragment in the four orientations illustrated in Figure 3.

Table 1. Structural Comparison between Molecular Mechanics Computed Structures (with the UFF) and Structural Parameters from the CSD

bond or angle	MM computed structure	CSD[a]	no. of CSD structures
average Re−C_{ring}	2.04 ± 0.09 Å	2.29 ± 0.04 Å	199
Re−P	2.53 ± 0.01 Å	2.43 ± 0.05 Å	1806
Re−N	1.992 ± 0.001 Å	1.76 ± 0.04 Å	207
Re−CH_2(olefin)	2.00 ± 0.04 Å	2.24 ± 0.07 Å	56
Re−C_{ipso}	2.28 ± 0.04 Å	2.26 ± 0.10 Å	56
Re−$C_{centroid}$(olefin)	2.04 ± 0.02 Å	2.13 ± 0.08 Å	56
N−O	1.10 ± 4 × 10^{-8} Å	1.19 ± 0.03 Å	207
C=C(olefin)	1.389 ± 0.001 Å	1.41 ± 0.04 Å	56
Re−N−O	179.3 ± 0.4°	174 ± 3°	207
Re−$C_{centroid}$−C_{ipso}	101 ± 5°		

[a] Structures from the CSD are all high-quality (R < 10%), monomeric complexes with no reported disorder and no reported errors.

Once bonded to the [CpRe(NO)(PPh_3)]$^+$ fragment, all the atoms in the olefin were fixed in their positions and the complex energy-minimized using the SMART minimizer.[34] By restraining the olefin, the [CpRe(NO)-(PPh_3)]$^+$ fragment is allowed to adjust to the conformation of the olefin. However, there is no guarantee that the conformation of the olefin in the two different fragments, $Cr(CO)_5$ and [CpRe(NO)(PPh_3)]$^+$, should be the same. Therefore, all olefin restraints were removed from the [CpRe(NO)$(PPh_3)(\eta^2$-olefin)]$^+$ complex, the P−Re−Centroid−C_{ipso} torsion angle was constrained to 0° or 180°, the C_{olefin}−Centroid−C_{olefin} atomic positions were fixed, and the structure was fully energy-minimized using the SMART minimizer. By fixing the olefinic position, we ensure the olefin remains in an orientation that matches the maximum overlap between HOMO and LUMO.[14]

Since we cannot run a methodical conformational search using the UFF on these systems, we chose molecular dynamics to refine the olefinic conformation. The complex was subjected to 1500 steps of constant NVT dynamics (500 K, 0.1 ps relaxation time, and dynamics time step of 0.001 ps) and fully energy-minimized. This final structure was used in the ligand repulsive energy calculation using ERCODE, which was developed in our laboratories.[25]

In general, the geometries of the complexes as computed with MM are internally consistent across all olefins studied. For example, the standard deviation for the cyclopentadienyl ring C−Re distance is 0.09 Å and the Re−N−O angle is 0.4°. The Cambridge Structural Database (CSD) was searched for high-quality (R < 10%), monomeric complexes with no reported crystallographic disorder and no reported errors. This search yielded 199 structures with Re and unsubstituted cyclopentadienyl ring, 1806 structures of Re-phosphines, 207 structures of Re-linear nitrosyls, and 56 structures with η^2-olefins coordinated to Re. There is reasonable agreement between MM computed structures and structural parameters from the CSD (Table 1), which is expected with the UFF calculations on organometallics.[2] The MM-computed Re−CH_2(olefin) distance is shorter (2.00 ± 0.08 Å) than the Re−C_{ipso}(olefin) distance (2.28 ± 0.04 Å). We expect this discrepancy since the *ipso* carbon of the olefin contains the substituent that experiences unfavorable steric interactions with the rest

(30) Rappé, A. K.; Casewit, C. J.; Colwell, K. S.; Goddard, W. A., III; Skiff, W. M. *J. Am. Chem. Soc.* **1992**, *114*, 10024−10035.
(31) Schilling, B. E. R.; Hoffmann, R.; Faller, J. W. *J. Am. Chem. Soc.* **1979**, *101*, 592.
(32) Kiel, W. A.; Lin, G.-Y.; Constable, A. G.; McCormick, F. B.; Strouse, C. E.; Eisenstein, O.; Gladysz, J. A. *J. Am. Chem. Soc.* **1982**, *104*, 4865.
(33) Czech, P. T.; Gladysz, J. A.; Fenske, R. F. *Organometallics* **1989**, *8*, 1810.
(34) The SMART minimizer first uses the steepest descent method to locate the approximate minimum and then switches to an adopted basis Newton−Raphson minimizer (first derivative method) and finally to the accurate truncated Newton method (combination of conjugate gradient and full Newton−Raphson second derivatives) to discard saddle points.
(35) *Cerius^2 4.5*; Molecular Simulations, Inc.: San Diego, CA, 2001.

Table 2. Ligand Repulsive Energies, E''_R (in kcal/mol), Total Molecular Mechanics Energies, E_i (in kcal/mol), Boltzmann-Weighted Total Molecular Mechanics Energies, w_i (in kcal/mol), Weighted Averaged Ligand Repulsive Energies, $\langle E''_R \rangle$, for CH_2=CHR Bonded to the $[CpRe(NO)(PPh_3)]^+$ Fragment

R	orientation[a]	E''_R	E_i[b]	w_i[c]	$\langle E''_R \rangle$[d]	experimental *RS,SR*:*RR,SS* ratio[14]	E_R[e]	E'_R[g]
Me	*RS,SR*	79	1239	0.999	0.999	95%	57	39
	*RS,SR*2	98	1245	4×10^{-5}	5×10^{-19}			
	RR,SS	89	1247	1×10^{-6}	6×10^{-14}			
	*RR,SS*2	91	2376	0.0	0.0			
n-Pr	*RS,SR*	82	1240	0.999	0.999	94%	58	39
	*RS,SR*2	110	1256	2×10^{-12}	6×10^{-33}			
	RR,SS	88	1253	3×10^{-10}	1×10^{-14}			
	*RR,SS*2	102	1246	4×10^{-5}	9×10^{-20}			
CH_2Ph (Bn)	*RS,SR*	81	1264	0.844	0.844	88%	75	
	*RS,SR*2	88	1265	0.156	1×10^{-6}			
	RR,SS	90	2071	0	0			
	*RR,SS*2	102	2070	0	0			
Ph	*RS,SR*	101	1276	0.999	0.999	93%	71	50
	*RS,SR*2	146	1283	7×10^{-6}	8×10^{-39}			
	RR,SS	125	1282	4×10^{-5}	1×10^{-22}			
	*RR,SS*2	154	1281	2×10^{-4}	3×10^{-43}			
i-Pr	*RS,SR*	92	1251	0.998	0.998	99%	69	49
	*RS,SR*2	108	1255	1×10^{-3}	2×10^{-15}			
	RR,SS	102	1256	2×10^{-4}	1×10^{-11}			
	*RR,SS*2	116	1256	2×10^{-4}	6×10^{22}			
t-Bu	*RS,SR*	99	1259	0.999	0.999	73%	83	55
	*RS,SR*2	128	1279	2×10^{-15}	1×10^{-36}			
	RR,SS	108	1271	2×10^{-9}	4×10^{-16}			
	*RR,SS*2	138	1272	3×10^{-10}	8×10^{-39}			
$SiMe_3$	*RS,SR*	92	1239	0.999	0.999	63%	64	43
	*RS,SR*2	124	1255	2×10^{-12}	7×10^{-36}			
	RR,SS	109	1249	5×10^{-8}	2×10^{-20}			
	*RR,SS*2	108	1264	5×10^{-19}	9×10^{-31}			

[a] See Figure 3 for orientation. [b] Computed with the UFF. [c] Computed using eq 2. [d] Computed with eq 3. [e] Computed with the $Cr(CO)_5$ fragment.[22] [f] Computed with the [CpRhCO] fragment.[22]

of the complex. Ideally, the Re−$C_{centroid}$(olefin)−C_{ipso} angle should be close to 90°. In the MM structures, this angle opens to an average of 101 ± 5° as a result of the aforementioned steric interactions. As the substituent on the olefin gets larger, the Re−$C_{centroid}$(olefin)−C_{ipso} angle deviates further from 90° (for example, this angle is 93.8° for the propene in the *RS,RS* orientation and 109.5° for CH_2=CH(*t*-Bu) in the *RS,SR* orientation).

Ligand Repulsive Energies, E_R'', with the $[CpRe(NO)(PPh_3)]^+$ Fragment. To ensure that the E_R'' values represent the steric demand of an olefin in the $[CpRe(NO)(PPh_3)]^+$ environment, we compare E_R'' to the ligand repulsive energies for η^2-bonded olefins in the literature.[22] Even though the conformationally flexible $[CpRe(NO)(PPh_3)]^+$ fragment is not ideal for the computation of ligand repulsive energies, there is remarkable agreement between the ordering of ligand repulsive energies computed with the $[CpRe(NO)(PPh_3)]^+$ fragment and the conformationally inflexible $Cr(CO)_5$ and CpRh(CO) fragments (Table 2). Excluding the benzyl datum, there is a good correlation between E''_R of the α-olefins in the *RS,SR* orientation computed with the $[CpRe(NO)(PPh_3)]^+$ fragment and E'_R values computed with the [CpRhCO] fragment ($r = 0.9$, see Table 2). There is also good agreement between E''_R of the olefins with the E_R values computed with the $Cr(CO)_5$ fragment ($r = 0.9$; Table 2).

The benzyl substituent is conformationally flexible and can adopt several low-energy conformations, each of which has a different ligand repulsive energy.[25] In particular, we find that the low-energy conformer of CH_2=CHBn is very different in the $Cr(CO)_5$, [CpRh(CO)], and $[CpRe(NO)(PPh_3)]^+$ fragments (Figure 4). The phenyl ring of the benzyl substituent in CH_2=CHBn is directed away from $Cr(CO)_5$ and $[CpRe(NO)(PPh_3)]^+$ (Figure 4a and c). However, the same phenyl ring is pointed toward the CpRh(CO) fragment (Figure 4b). All three complexes are low-energy structures, but the ligand repulsive energies are dramatically different as a result of the phenyl ring conformation (Table 2). We chose to exclude the benzyl datum from correlations with E''_R because the conformations are so different in the three different prototypical environments. None of the other olefinic substituents show as dramatic a conformational change upon moving between fragments.

The correlations between E''_R for the other three isomers in the $[CpRe(NO)(PPh_3)]^+$ environment and E_R values are poor ($r = 0.6-0.8$). Since the *RS,SR* isomer contains the olefin in the least sterically demanding orientation (Figure 3), we expect the least interligand gearing, giving rise to ligand repulsive energy trends that closely match the less sterically demanding $Cr(CO)_5$ and [CpRh(CO)] fragments. The good correlation between E''_R computed for the olefins in the *RS,SR* orientations and E_R values is a further indication that ligand repulsive energies are a robust measure of steric bulk and their trends are relatively fragment-independent.

The magnitudes of E''_R in the $[CpRe(NO)(PPh_3)]^+$ environment are larger than those for the $Cr(CO)_5$ and [CpRh(CO)] fragments, which implies that $[CpRe(NO)(PPh_3)]^+$ is the most sterically demanding of the three.[22] The ligand repulsive energies for the α-olefins in the $[CpRe(NO)(PPh_3)]^+$ environment increase *RS,SR* < *RS,SR*2 and *RR,SS* < *RR,SS*2. Therefore, we may conclude that the steric crowding between metal fragment and olefin in *RS,SR*2 and *RR,SS*2 isomers is more

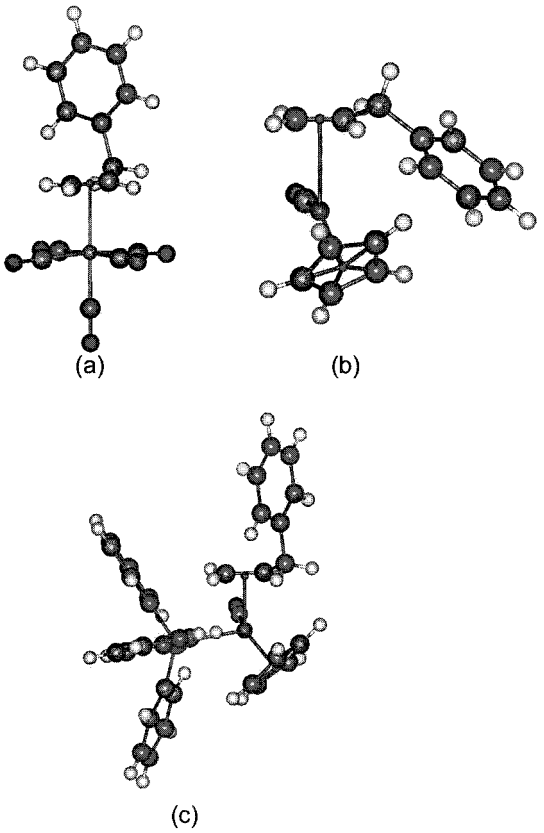

Figure 4. (a) $[Cr(CO)_5(\eta^2\text{-}CH_2{=}CHBn)]$. (b) $[CpRh(CO)(\eta^2\text{-}CH_2{=}CHBn)]$. (c) $[(\eta^5\text{-}C_5H_5)Re(\eta^2\text{-}CH_2{=}CHBn)(PPh_3)(NO)]^+$. Note the different conformation of the benzene ring of the benzyl substituent on moving fragments from $Cr(CO)_5$ to $[CpRh(CO)]$ to $[CpRe(NO)(PPh_3)]^+$.

pronounced than the olefin in the *RS,SR* and *RR,SS* orientations, as expected.

For the series of α-olefins $CH_2{=}CHR$ (R = Me, *n*-Pr, CH_2Ph (Bn), Ph, *i*-Pr, *t*-Bu, and $SiMe_3$), Gladysz has shown experimentally that the olefin coordinates to form the *RS,SR* isomers preferentially over the *RR,SS* isomers (Figure 3).[14] In each case, our computations show that E_R'' for the *RS,SR* isomer is lower than that of the *RR,SS* isomer, which agrees with experiment (see Table 2). We do not expect the magnitude of the difference in E_R'' between *RS,SR* and *RR,SS* isomers to correlate with the experimental selectivity, since these ligand repulsive energies need to be weighted by the internal energy of the isomer in order to produce a parameter that is related to the experimental diastereoselectivity, de.

The total molecular mechanics energies of complexes with the olefins in the *RS,SR* orientation consistently have the lowest MM energies for a given substituent (see Table 2). However, it is possible for a conformer with a low E_R'' to overcome the higher energy penalty and still dominate in a reaction. Therefore, we need to define a Boltzmann weight for isomer *i*, w_i, in terms of the difference in molecular mechanics energy, $E_i - E_0$, where E_i is the energy of isomer *i* and E_0 is the energy of the lowest energy isomer for a given olefin:

$$w_i = \frac{\exp\left(-\frac{E_i - E_0}{kT}\right)}{\sum \exp\left(-\frac{E_i - E_0}{kT}\right)} \qquad (2)$$

In eq 2, *k* is the Boltzmann constant and *T* is taken as 298.15 K ($kT = 0.592476141388$ kcal/mol at 298.15 K). To compare the selectivities of different fragments (see below), we need to be careful to include E_R'' in such a way so that we can compare E''_R across the different fragments. Therefore, we define $\langle E_R''\rangle_i$ for isomer *i* as

$$\langle E''_R\rangle_i = w_i \exp\left(-\frac{\Delta E''_R}{kT}\right) \qquad (3)$$

where $\Delta E''_R$ is the E''_R for isomer *i* minus the lowest E''_R across all isomers. We can define a computed diastereoselectivity, de_{MM}, as

$$de_{MM} = (\langle E_{RS,SR}\rangle + \langle E_{RS,SR2}\rangle) - (\langle E_{RR,SS}\rangle + \langle E_{RR,SS2}\rangle) \qquad (4)$$

where $\langle E_{RS,SR}\rangle$ is the $\langle E''_R\rangle_i$ for the *RS,SR* isomer, etc. When we plot de_{MM} against experimentally determined de, we find that the benzyl datum is a significant outlier. Once removed, de_{MM} values still do not correlate with experimental de ($r = 0.50$), which implies that the total molecular mechanics energy is not an adequte representation of the total internal energy for the conformer.

We compute a diastereoselectivity based on total molecular mechanics energy alone by replacing $\langle E''_R\rangle_i$ in eq 4 with w_i, which also does not correlate well with experimental de ($r = 0.54$), for the same reason as noted above. Finally, it is possible to compute a de based on E''_R alone using expressions analogous to eqs 2 and 4. In this case, the computed de does not correlate with the experimental de ($r = 0.25$), so we do not consider this metric any further. The most sound comparison between computationally derived quantity and experimental de is to weight E''_R, which is a good quantitative measure of steric effects, with the total internal energy as computed by SEQM or DFT methods (eqs 2−4). These computations are currently underway in our laboratory.

In Table 2, we note that E''_R for the *RS,SR* isomers are all lower than those for the *RS,SR*2 isomers. We anticipate a higher E''_R for the *RS,SR*2 isomer since this isomer places the olefinic substituent in the interstice between the bulky PPh_3 and Cp ligands (**B** in Figure 3). Similarly, the *RR,SS* isomers also have lower ligand repulsive energies than the *RR,SS*2 isomers with the exception of $SiMe_3$, which shows approximately the same E''_R for both **C** and **D** (Table 2). Gladysz argued that the correct stereoisomer can be predicted by knowing the relative steric crowding of the different interstices between ligands on the metal. He reasoned that the olefinic substituent is directed into the least sterically hindered interstice, Figure 2.[14]

The E''_R results described above confirm Gladysz's hypothesis that the stereoselective binding of prochiral α-olefins to $[CpRe(NO)(PPh_3)]^+$ can be understood using a steric argument. Now, we turn our attention to examining the effect of changing the steric demand of the ligands on the binding of the same set of prochiral α-olefins.

Ligand Repulsive Energies with the $[CpRe(NO)(PMe_3)]^+$, $[Cp^*Re(NO)(PMe_3)]^+$, and $[Cp^*Re(NO)(PPh_3)]^+$ Fragments. The relative ordering of cone angles[16,20] of the ligands we consider is Cp* ($\theta = 182°$) > PPh_3 ($\theta = 145°$) > Cp ($\theta = 128°$) > PMe_3 ($\theta = 118°$)

Table 3. Ligand Repulsive Energy Data, E''_R (in kcal/mol), and Weighted Averaged Ligand Repulsive Energies, $\langle E''_R \rangle$, for CH_2=CHR Bonded to the $[CpRe(NO)(PMe_3)]^+$, $[Cp^*Re(NO)(PMe_3)]^+$, and $[Cp^*Re(NO)(PPh_3)]^+$ Fragments

		$[CpRe(NO)(PMe_3)]^+$		$[Cp^*Re(NO)(PMe_3)]^+$		$[Cp^*Re(NO)(PPh_3)]^+$	
R	orientation	E''_R	$\langle E''_R \rangle$	E''_R	$\langle E''_R \rangle$	E''_R	$\langle E''_R \rangle$
Me	*RS,SR*	65	0.983	77	0.999	90	0.286
	*RS,SR*2	74	1×10^{-8}	81	8×10^{-7}	105	3×10^{-17}
	RR,SS	76	4×10^{-13}	86	7×10^{-17}	89	4×10^{-10}
	*RR,SS*2	79	1×10^{-14}	88	3×10^{-14}	110	4×10^{-22}
n-Pr	*RS,SR*	69	0.999	79	0.996	90	0.994
	*RS,SR*2	85	6×10^{-35}	86	3×10^{-8}	107	4×10^{-15}
	RR,SS	77	5×10^{-15}	94	2×10^{-32}	99	5×10^{-25}
	*RR,SS*2	82	3×10^{-17}	93	6×10^{-15}	142	4×10^{-22}
CH_2Ph (Bn)	*RS,SR*	68	0.998	76	0.983	95	0.999
	*RS,SR*2	76	3×10^{-9}	87	8×10^{-11}	119	3×10^{-22}
	RR,SS	77	1×10^{-13}	87	3×10^{-18}	97	9×10^{-14}
	*RR,SS*2	83	1×10^{-15}	94	3×10^{-17}	117	3×10^{-22}
Ph	*RS,SR*	91	0.993	116	0.120	121	0.997
	*RS,SR*2	114	1×10^{-19}	118	6×10^{-9}	145	1×10^{-25}
	RR,SS	109	1×10^{-17}	115	1×10^{-9}	145	2×10^{-24}
	*RR,SS*2	116	1×10^{-22}	129	4×10^{-15}	166	8×10^{-36}
i-Pr	*RS,SR*	83	0.961	101	0.229	98	0.999
	*RS,SR*2	104	5×10^{-25}	100	1×10^{-5}	119	5×10^{-28}
	RR,SS	85	1×10^{-4}	100	7×10^{-11}	108	7×10^{-23}
	*RR,SS*2	98	8×10^{-15}	107	7×10^{-11}	129	1×10^{-32}
t-Bu	*RS,SR*	88	0.999	106	0.130	114	0.500
	*RS,SR*2	112	2×10^{-23}	120	6×10^{-27}	141	6×10^{-31}
	RR,SS	94	6×10^{-16}	105	5×10^{-19}	114	6×10^{-16}
	*RR,SS*2	114	1×10^{-57}	118	2×10^{-20}	153	2×10^{-39}
$SiMe_3$	*RS,SR*	76	0.999	91	0.999	101	1.00
	*RS,SR*2	97	1×10^{-19}	102	5×10^{-18}	133	1×10^{-35}
	RR,SS	86	2×10^{-14}	100	2×10^{-21}	109	2×10^{-18}
	*RR,SS*2	99	3×10^{-25}	112	1×10^{-23}	142	4×10^{-42}

> NO. (The cone angle of CO is 90°, and the cone angle of NO is unreported.[16] We assume that the cone angle of NO is close to 90°.) As a consequence of this relative ordering of cone angles, we expect all fragments to be selective toward the same olefinic face. The only isomers that are affected by the change in phosphine are *RS,SR*2 and *RR,SS*2, which are not important in determining selectivity (Table 3). Since the ligand repulsive energies for the *RS,SR*2 and *RR,SS*2 isomers are generally higher than those for the *RS,SR* and *RR,SS* isomers (Table 3), and since de_{MM} is dominated by the isomer with the lowest E''_R, we expect that changing the phosphine will not alter the *direction* of stereoselectivity.

Because of the different relative sizes of Cp and Cp* versus PMe_3 and PPh_3, we expect moving from Cp to Cp* keeping the phosphine constant should have a greater effect on selectivity than changing phosphines keeping the Cp ring size constant. However, molecular mechanics geometries are often perturbed by the introduction of the bulky Cp* ligand, which results in an opening of the $Cp^*_{centroid}$−Re−P angle. For example, the average $Cp^*_{centroid}$−Re−P angle is 128° for $[Cp^*Re(NO)(PPh_3)]^+$, whereas the average $Cp_{centroid}$−Re−P angle in $[CpRe(NO)(PPh_3)]^+$ is 121° (Figure 5).

As a consequence of opening the Cp−Re−P angle, the olefin in the *RR,SS*2 orientation of $[Cp^*Re(NO)(PPh_3)]^+$ (Figure 3) shows a greater E''_R than in the anticipated *RS,SR*2 orientation. This relative crowding of the *RR,SS*2 orientation is reflected in the E''_R values in Table 3. Increased steric repulsion between olefin in the *RS,SR*2 and *RR,SS*2 orientations *does not result in a consistently better and uniform selectivity*.

The $[CpRe(NO)(PMe_3)]^+$ complexes **B** and **D** (Figure 3) have the olefin in a less congested environment compared to the $[CpRe(NO)(PPh_3)]^+$ fragment. Consequently, the relative size of E''_R for the olefins in **B** and **D** are lower for L = PMe_3 than PPh_3 (Table 3). All ligand repulsive energies for the $[CpRe(NO)(PMe_3)]^+$ fragment are lower than the E''_R values for $[CpRe(NO)(PPh_3)]^+$ because of the smaller size of the PMe_3 ligand.

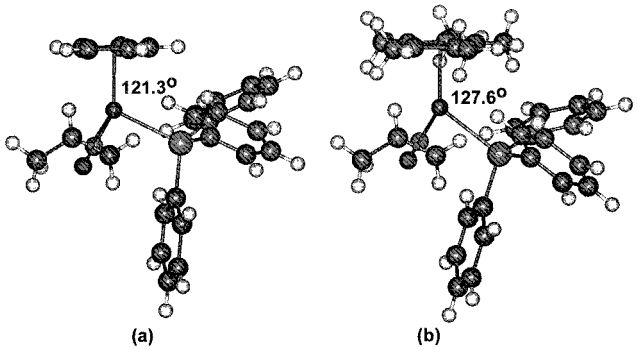

Figure 5. (a) $[(\eta^5\text{-}C_5H_5)Re(\eta^2\text{-}CH_2{=}CHMe)(PPh_3)(NO)]^+$. (b) $[(\eta^5\text{-}C_5Me_5)Re(\eta^2\text{-}CH_2{=}CHMe)(PPh_3)(NO)]^+$. The $Cp_{centroid}$−Re−P bond angle is 121° in (a) and 128° in (b). Both complexes are shown in the least sterically hindered *RS,SR* orientation.

There is better agreement between ligand repulsive energies in the $[CpRe(NO)(PMe_3)]^+$ environment and previously reported E_R values ($r = 0.9-0.94$) than with the $[CpRe(NO)(PPh_3)]^+$ fragment. This improvement is also anticipated since the $[CpRe(NO)(PMe_3)]^+$ environment is less congested than $[CpRe(NO)(PPh_3)]^+$, which makes $[CpRe(NO)(PMe_3)]^+$ more *sterically similar* to $Cr(CO)_5$ and [CpRh(CO)].

The ratio of *RS,SR* to *RS,SR*2 ligand repulsive energy provides information about the relative congestion difference when the olefin is located in different interstices between the ligands (**A** and **B** in Figure 3). In the case of the $[CpRe(NO)(PPh_3)]^+$ fragment, the *RR,SS*:*RR,SS*2

ligand repulsive energy ratio (0.795) is greater than the *RS,SR*:*RS,SR*2 ratio (0.892), which implies that the difference between orientations **A** and **B** (Figure 3) is more dramatic than between **C** and **D**. The same trend in E_R'' is seen with the $[CpRe(NO)(PMe_3)]^+$ fragment, only to a lesser degree (0.854 for *RS,SR*:*RS,SR*2 and 0.907 for *RR,SS*:*RR,SS*2), which implies the $[CpRe(NO)(PMe_3)]^+$ fragment is less selective than the $[CpRe(NO)(PPh_3)]^+$ fragment.

Even though we know that total molecular mechanics energy is a poor representation of the total internal energy of the system, we compute a de_{MM} using eq 4 in order to compare the selectivities of the different fragments. Although we do not anticipate that these selectivities will correlate with experiment, we do expect them to be internally consistent since steric effects are well-represented in molecular mechanics.[26] In other words, the de_{MM} values computed for the different fragments reflect the relative ability of a fragment to stereoselectively bind a prochiral α-olefin. Since the benzyl datum is a clear outlier in the plot of experimental de versus de_{MM}, we chose to exclude benzyl from all comparisons of average de_{MM}.

The average selectivity, de_{MM}, for the $[CpRe(NO)(PPh_3)]^+$ fragment is 0.9997, whereas average de_{MM} for the $[CpRe(NO)(PMe_3)]^+$ fragment is 0.989, which supports the conclusion above that the $[CpRe(NO)(PPh_3)]^+$ fragment is more selective than the $[CpRe(NO)(PMe_3)]^+$ fragment. In addition, the $[CpRe(NO)(PMe_3)]^+$ fragment selectively coordinates the same face of a prochiral olefin as the $[CpRe(NO)(PPh_3)]^+$ fragment, which is indicated by the sign of de_{MM} in eq 4.

For the $[Cp^*Re(NO)(PMe_3)]^+$ fragment, E''_R for the *RS,SR* isomers are lower than those for the *RS,SR*2 isomers for all olefins except styrene. The E''_R values for the $[Cp^*Re(NO)(PMe_3)]^+$ fragment are lower than we would expect on the basis of the differences in cone angles of the ligands as a result of the geometric deformation resulting from the bulk of the Cp* ligand (Figure 5). In almost all cases, the ligand repulsive energies are higher for $[CpRe(NO)(PPh_3)]^+$ than for $[Cp^*Re(NO)(PMe_3)]^+$. This implies that an α-olefin experiences less steric congestion in a complex with $[Cp^*Re(NO)(PMe_3)]^+$ than with $[CpRe(NO)(PPh_3)]^+$ even though the cone angles of the ligands do not reflect this difference. Consequently, the selectivity of the $[Cp^*Re(NO)(PMe_3)]^+$ fragment ($de_{MM} = 0.579$) is worse than that for the $[CpRe(NO)(PPh_3)]^+$ fragment. (If the styrene datum, for which the olefin in the *RR,SS* isomer has a lower E''_R than in the *RS,SR* isomer, is omitted, then average de_{MM} for the $[CpRe(NO)(PMe_3)]$ fragment is 0.897.)

When we compare average de_{MM} values for $[CpRe(NO)(PMe_3)]^+$ to $[Cp^*Re(NO)(PMe_3)]^+$, we find that de_{MM} is *lower for the more bulky fragment* (0.989 vs 0.579). This selectivity differential implies that the size of the phosphine is more important than the size of the cyclopentadienyl ring in stereoselectively binding a prochiral olefin.

The $[Cp^*Re(NO)(PPh_3)]$ fragment shows trends in E''_R values analogous to the $[Cp^*Re(NO)(PMe_3)]^+$ fragment, as expected. The average de_{MM} value for the $[Cp^*Re(NO)(PPh_3)]^+$ fragment is 0.796, with all selectivities occurring toward the *RS,SR* face of the olefin, as expected.

It is important to emphasize that the direction of the selectivity is significant in the molecular mechanics model. To obtain a computational model of de, a good representation of the total internal energy is required. However, since steric effects are well represented in MM but not as well represented in SEQM or ab initio methods, we will need to retain the MM-based E''_R as a quantitative measure of steric effects in these systems.

Summary and Molecular Mechanics-Based Ligand Design Criteria. We have managed to understand the experimental binding selectivity of $[CpRe(NO)(PPh_3)]^+$ toward prochiral α-olefins using a molecular mechanics-based steric model. The direction of our computed selectivities agrees with experiment in all cases. On the basis of this agreement, we have examined the steric interplay between ligands on Re and the substituent on the prochiral α-olefin in order to rank the relative importance of the sizes of ligands in terms of binding selectivities. From these molecular mechanics results, we may conclude that the size of the phosphine appears more important than the size of the cyclopentadienyl ring in determining which face of a prochiral olefin is bound by an enantiomerically pure organometallic Lewis acid. We are in the process of continuing up the de novo design pyramid by examining the sterics and energetics of the system using semiempirical quantum mechanical calculations.

Acknowledgment is made to the donors of the Petroleum Research Fund, administered by the American Chemical Society, for support of this research. Funding for this project was also provided by the NSF through grant CHE-0111131. We thank Elizabeth A. Downing for work with some preliminary data and Professor Thomas R. Cundari, University of Memphis, for useful discussions during the revision of the manuscript.

OM010481A